

## HIGH RESOLUTION THERMAL MAPPING OF MICROCIRCUITS USING NEMATIC LIQUID CRYSTALS

G. ASZÓDI†, J. SZABON, I. JÁNOSSY and V. SZÉKELY‡

Liquid Crystal Department, Central Research Institute for Physics, H-1525 Budapest, P.O.B. 49, Hungary

(Received 25 September 1980; in revised form 1 June 1981)

**Abstract**—An improved method for high resolution thermal mapping is discussed. This method utilizes nematic liquid crystals and has been primarily applied to inspect microcircuits. By making use of two nematic liquid crystals in conjunction with reflected light polarizing microscopy a thermal resolution of about 0.05 K has been achieved. Resolution limits are considered in detail for heat generation occurring at some depth from the surface of the sample. In addition, a comparison is made between the commonly used cholesteric method and the present work.

To demonstrate the capability of the method the thermal mapping of an LED is shown.

### NOTATION

$K$	thermal conductivity, W/mK
$d, D, r, \eta, \xi$	distances, mm
$x, y, z$	Cartesian coordinates,
$p$	dissipation density, W/m <sup>2</sup>
$T$	absolute temperature, K
$\nabla T$	temperature gradient, K/mm

### INTRODUCTION

The application of cholesteric liquid crystals to thermal mapping has become widespread during the past 20 years [1, 2]. Many applications can be found in microelectronics, e.g. microwave devices, thermally activated information displays or fault location [2]. However, use of cholesterogens in making thermal maps of microcircuits (even with more refined experimental arrays) fails to solve the fundamental problem of temperature and spatial identification of the surface isotherms [3]. Recent use of a complex experimental method for thermal mapping of microwave integrated circuits has enabled us to achieve a 0.1 K thermal and 50  $\mu$ m spatial resolution. However, the resolution is strongly influenced by the surface thermal gradient and precise evaluation is not simple.

To overcome all these and other difficulties we discuss here an experimental method that utilizes nematic liquid crystal temperature detector layers as described by Stephens and Sinnandurai [4]. They used the so called clearing point phase transition of a nematogen to indicate hot spots in integrated microcircuits. A recent application of the method is in the temperature profile measurement along a thick film resistor [5]. Here the isothermal lines are spatially distinguishable within 5  $\mu$ m, and the corresponding temperature can be measured with an accuracy of 0.5 K. The scope of the present work is (i) To improve the accuracy of determining iso-

therms and to consider the applicability to very small surface thermal gradients.

(ii) To analyse the resolution and error of the measurements when heat sources are at some depth from the surface.

(iii) To study the effect of a detector layer covering the sample surface.

(iv) To examine the nematogen detector material properties.

Points (i), (iv) and (ii), (iii) will be considered in detail in Section 1 and in the appendix, respectively.

### EXPERIMENTAL

#### Materials

A mixture of two mesogens (BDH, England) was used, viz. octyloxy-cyanobiphenyl, 8OCB (BDH name M24) and octyl-cyanobiphenyl, 8CB (BDH name K24). The phase transition temperature was measured by differential scanning calorimetry (DSC) and by using a polarizing microscope with a hot stage giving an accuracy to within  $\pm 0.05$  K. A Perkin-Elmer DSC-2 enables the impurity content to be determined thermoanalytically (for details see Ref. [6]).

The sensitivity of the "clearing transition" of a liquid crystalline compound to impurity content (due to water absorption, airborne contamination, etc.) was apparent from earlier studies. A small amount (0.5–0.8%) of impurities can

(a) Depress the clearing point,  $T_c$ .

(b) Broaden the phase transition temperature region [7].

Because of the close relationship and similar polar character of the homologues (8CB and 8OCB), their mixtures behave ideally (Fig. 1). The nematic-isotropic transition remains sharp and independent on concentration; the DSC thermograms do not indicate any broadening (Fig. 3a—fresh sample). As a result, an optimal mixture of clearing temperature ( $T_c$ ) closest to the temperature range studied could be selected (see Fig. 1).

†Department of Semiconductors, Research Institute for Technical Physics, H-1325 Budapest, Ujpest 1, P.O.B. 76, Hungary.

‡Chair for Electron Devices, Technical University of Budapest, H-1521 Budapest, Hungary.

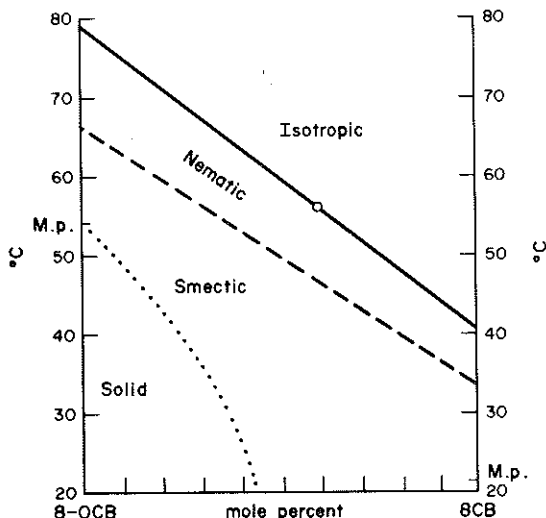


Fig. 1. Transition temperature of 8-OCB-8CB mixtures as a function of concentration (in mole per cent). Nematic-isotropic transitions: solid line; smectic-nematic transitions: dashed line; melting: dotted line (circle: transition temperature of 60 mole per cent 8CB in 8-OCB).

The effect of the thermal gradient on the sharpness of the  $T_c$  line was examined as a function of varying degrees of contamination of the materials. Whenever a thermal gradient is generated on a surface whose temperature is near to the  $T_c$  of the cover material, a sharp straight border-line would separate the nematic phase from the warmer isotropic phase unless the thermal gradient is less than 0.05–0.10 K per 1000  $\mu\text{m}$  (Fig. 2a). In the latter case an “archipelago” of nematic droplets arises whose width depends on the contamination of the material (and, of course, on the thermal gradient). In other words, sharpness fades due to excessive contamination, as illustrated in Fig. 2(b) ( $T_c$ -broadening). Contamination (degradation) of the mixtures used was followed by DSC. After ten weeks of application the clearing point was changed by 0.05 K only and the transition broadened somewhat (from 0.08 to 0.45 K, Fig. 3b). Due to intentional “carelessness” (container kept open for weeks) the clearing point depression was only 0.2 K but the width of the transition line increased by an order of magnitude (Fig. 3c).

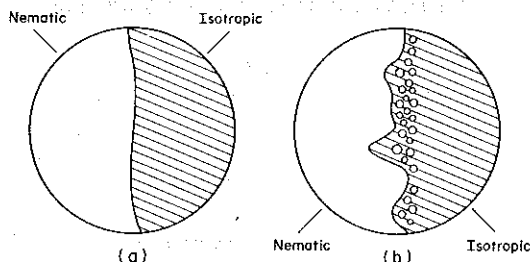


Fig. 2. Illustration of the effect of thermal gradient on the sharpness of the boundary ( $T_c$  isothermal line): (a)  $\nabla T$  is not less than 0.1 K per 1000  $\mu\text{m}$ ; (b)  $\nabla T$  less than 0.05–0.10 K per 1000  $\mu\text{m}$ , fresh sample.

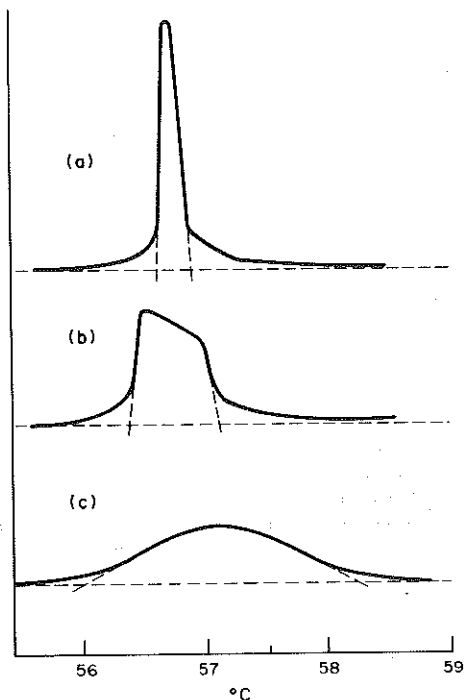


Fig. 3. Broadening of transitions: DSC traces of nematic-isotropic transition of samples (containing 60% 8CB) of varying contamination. (a) fresh sample; (b) sample after 60 days of application; (c) excessive contamination due to prolonged absorption (sample open for weeks).

## 2. Sample preparation

DSC measurements show that the method of using solvents for producing thin (5  $\mu\text{m}$ ) films of nematogens [4] can cause a change in the  $T_c$  value. This is possibly due to some of the solvent remaining in the material. Moreover, once the nematic layer has melted above its clearing point it condenses into droplets depending on the wetting power of the given substrate. To avoid this, we produced the detector layer simply by melting it above the transition temperature. Excess liquid crystals were removed from the surface of the sample by inert gas flow.

## 3. Experimental setup

A detailed scheme of the experimental apparatus used is given in Ref. [4]. Here, a thermostable sample holder is used together with an ultra-thermostat type U-10 (VEB MLW Medingen, GDR) with a maximum stability of 0.1 K. The holder is from copper isolated thermally from the outer space but in good thermal contact with the sample holder (usually TO-5 or TO-18 Covar headers).

For easy and good observation of the microcircuits we used “Amplival pol-u” microscope (Carl-Zeiss, Jena) in reflection mode with an “mf-matic” microphotographic research accessory. To eliminate possible heating effects of the sample we utilized KG-2 colour glass heat filters (Carl-Zeiss, Jena). Magnification was up to 200. With crossed polarizer and analyser, we could easily distinguish the different phases.

## 4. An experimental example: thermal mapping of an LED

The example given here is the thermal mapping of a chip (approx. 600  $\times$  600  $\mu\text{m}$ ) from a commonly manufac-

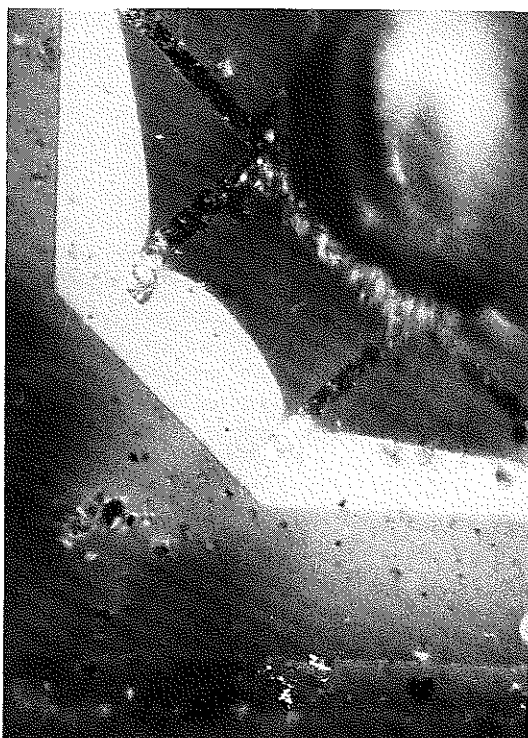


Fig. 5. Original photomicrograph of part of a LED with octagonal dissipation area. The isotherm corresponding to 31.9 K is the boundary of the nematic-isotropic regions. Using a polarized incident light beam the isotropic region is the dark one. The evaporated Au-contacts can also be seen. Due to the higher current density (dissipation) near the contacts, the surface is at higher temperature there.

tured LED with an octagonal active area whose parallel sides are at a distance of  $400\ \mu\text{m}$ . To introduce current from the front we utilized two pairs of parallel, vacuum-evaporated contact strips, perpendicular to each other. At the crossing of the contacts a rectangular contact acts as the connection to a  $25\ \mu\text{m}$  dia. gold wire. The chip contains a  $p$ - $n$  junction on a GaP substrate. The dimensions and the construction can be seen in Fig. 4. The depth of the  $p$ - $n$  junction was several  $\mu\text{m}$  from the upper surface of the LED. (For a detailed analysis of the physics and technology of LEDs see, for example, Ref. [8].)

In analysing the electrical resistivity of the main elements (i.e. GaP substrate, Covar header, epitaxial layers, gold contacts) of the LED one can see that the main part of the dissipated power arises from the  $p$ - $n$  junction region. A comparison of the appropriate thermal conductivities enables us to estimate the difference in temperature between the junction and the surface. The detailed analysis in the appendix shows that the difference in temperature is much less than  $0.01\ \text{K}$ . Thus, the liquid crystal layer on the surface of the sample enables us to measure the  $p$ - $n$  junction temperature. The "heating map" of the chip with a given electrical driving power as a parameter is illustrated in Fig. 5; this is a photomicrograph of an LED with a well-observable phase transition trajectory. For the sake of clarity only one isotherm is given. Figure 6(a) is the complete map of the same sample in the temperature range  $31.5$ – $32.5^\circ\text{C}$  with equidistant temperature increments of  $0.1\ \text{K}$ . The widths of the isothermal lines are uniform within  $2$  to  $4\ \mu\text{m}$ , as can be seen on the original photograph (Fig. 5). To simulate the thermal properties of the LED in question (i.e. the isotherms corresponding to a given input power) we applied the computer program THERMANAL [9]. In Fig. 6(b) the shape of the thermal map and the relative differences in temperature between isotherms correspond to a dissipated power of  $1\ \text{W}$ .

#### DISCUSSION

In the previous sections it was shown that the applicability of nematic liquid crystal thermography can be extended by considering some theoretical and experimental problems in detail. The high resolution temperature maps of the LED show that the method works even with a very small temperature gradient. To indicate the isotherms we used the so called clearing point phase transitions of the nematogen—as described in the literature [4]. Our examinations have shown that the

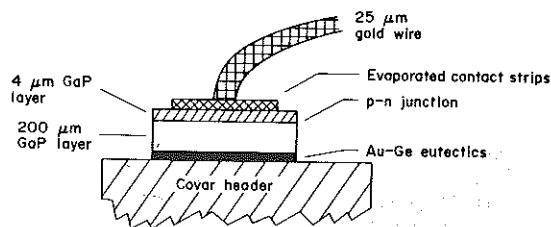
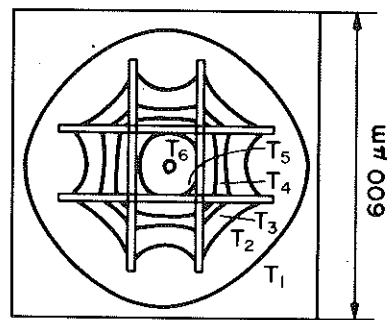
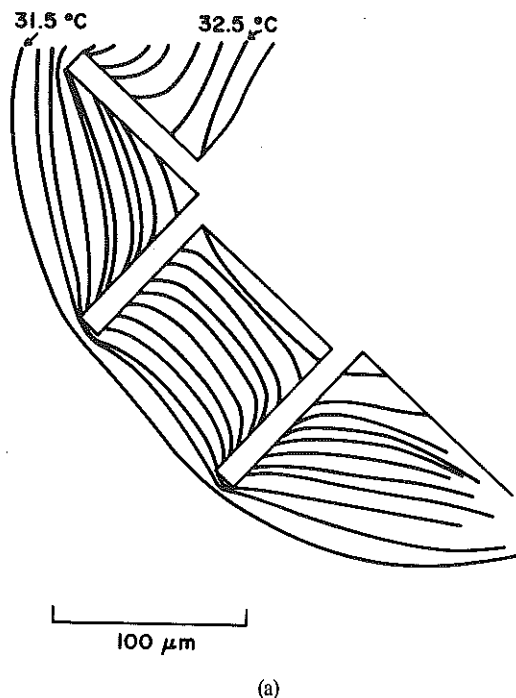


Fig. 4. Scheme of LED. (Details not important from a viewpoint of thermodynamics are not represented; dimensional outlines are not to scale.)



$T_0 = 25^\circ\text{C}$			$P_{\text{INPUT}} = 1\ \text{W}$		
$T_1 = 26^\circ\text{C}$	$T_2 = 28^\circ\text{C}$	$T_3 = 30^\circ\text{C}$			
$T_4 = 32^\circ\text{C}$	$T_5 = 36^\circ\text{C}$	$T_6 = 38^\circ\text{C}$			

(b)

Fig. 6. (a) Complete temperature map of the same part of LED as shown in Fig. 5 and constructed from eleven photographs. For the sake of clarity only the outermost and innermost isotherms are marked with their temperature values. The temperature difference between two consecutive lines is  $0.1\ \text{K}$ . Dissipated power was  $0.38\ \text{W}$ . (b) Computer simulation for the thermal map of LED. (For technical parameters, see text.) Dissipated power was  $1\ \text{W}$ .

smectic-A–nematic phase transition cannot precisely localize the corresponding isotherms, presumably due to the strong pre-transitional effects near the transition. Use of the method may well be beneficial for the thermal mapping of high power microcomponents. Important physical parameters such as thermal conductivity, thermal resistance, active layer temperature can be measured even in the case of multilayer structures using the method detailed above. Some of the results obtained will be published elsewhere.

**Acknowledgements**—The authors wish to thank Dr. L. Bata, Liquid Crystal Research Group, Central Research Institute for Physics, Budapest, for helpful discussions.

**REFERENCES**

1. P. Caroll, *Cholesteric Liquid Crystals. Their Technology and Applications*. Ovum Ltd., London (1973).
2. G. Meier, E. Sackmann and J. G. Grabmeier, *Applications of Liquid Crystals*. Springer Verlag, Berlin (1975).
3. F. Gianni, P. Maltese and R. Sorrentino, *Appl. Optics* **18**, 3048 (1979).
4. C. E. Stephens and F. N. Sinnandurai, *J. Phys. E: Scient. Instru.* **7**, 641 (1974).
5. F. N. Sinnandurai, *Electrocomponent Science and Technology* **6**, 177 (1980).
6. L. Siklos and J. Szabon, In *Adv. in Liq. Crys. Res. Appl.* (Edited by L. Bata), coedition of Akadémiai Kiadó, Budapest and Pergamon Press, Oxford (1981).
7. J. Szabon, L. Bata and K. Pintér, KFKI-Preprint, KFKI-1978-22 (1978).
8. *Proc. Int Autumn School Semicond. Optoelectronics, Semicond. Sources of El.magn.Radiation* (Edited by Marian A. Herman), Warszawa, Polish Scientific Publications (1976).
9. V. Székely, P. Baji and M. Kerecsen, A display-interactive program for simulation of heat distribution of IC-chips. *Vth Hungarian Conf. Elect. Measur. Equip.*, (in Hungarian) Budapest (1980).
10. H. S. Carslaw and J. C. Jaeger, *Conduction of Heat in Solids*. Oxford University Press, Oxford, England (1959).

**APPENDIX**

Our measurements show that in general the LED surface temperature vs the surface coordinates varies only slowly. We have used the well-known method of thermal resistivity to calculate temperature differences between the surface and the *p-n* junction. From the experimental point-of-view it is negligible (less than 0.01 K) but this is not so if point-type heat sources exist. We calculated theoretically the resolution of our method if heat sources of such a type are included.

In our case the main component of the heat source (e.g. a *p-n* junction) is not exactly at the semiconductor surface but rather at some depth from it. Thus the temperature reaches its maximum value in the bulk, at a given distance from the surface, whereas the described method measures surface temperatures only. The surface temperature distribution is a finite resolution image of the deep-distribution with different maximum temperature values. This leads to the questions:

- (i) What is the error, i.e. the temperature difference, between the exact temperature maximum and the measured one?
- (ii) To what extent is spatial resolution limited by the dissipating sources being below the surface?

**Model for discussion.** Let us investigate the steady-state temperature distribution of the sample. This is given by the stationary heat-conduction eqn[10].

$$\nabla^2 T = 0. \tag{A1}$$

For a point-source the solution of (A1) is given by

$$T(r) = \frac{1}{4\pi K} \frac{1}{r} \tag{A2}$$

where *K* is the thermal conductivity of the medium and *r* is the distance from the source.

The neighbourhood of the semiconductor surface is a two-region structure: one region is the semiconductor itself, the other is the air above it. The thermal conductivity of the air is *K* = 0.024 W/mK. This is four orders of magnitude smaller than that of the semiconductor (e.g. 155 W/mK for silicon). (On the other hand the liquid crystal used for thermography has a thermal conductivity of about  $1.5 \times 10^{-1}$  W/mK, that is, three orders of magnitude smaller than that of the silicon.) Thus, the thermal

conductivity of the air (or the liquid crystal) can be completely neglected. Radiation is also negligible and air convection is prevented during the test. The heat propagates only in the semiconductor material, so we can use the semi-infinite medium approximation. In this approximation the volume temperature distribution is given from (A2) by a convolution-type integral

$$T(x, y, z) = \frac{1}{4\pi K} \sum_{i=0}^1 \int \frac{p(\xi, \eta)}{\sqrt{((x-\xi)^2 + (y-\eta)^2 + [z+(2i-1)d])^2}} d\xi d\eta \tag{A3}$$

where *p*( $\xi, \eta$ ) is the two-dimensional dissipation density at a depth *d* from the surface.

**Error of measurements of maximum temperature.** For a circular dissipation area with diameter *D* (Fig. 7a) and uniform dissipation density *p*, eqn (A3) gives the maximum bulk temperature as

$$T_B = \frac{p}{2K} \left( \frac{D}{2} + \sqrt{\left(\left(\frac{D}{2}\right)^2 + (2d)^2\right) - 2d} \right) \tag{A4}$$

referring to point *B* in Fig. 7(a). The maximum surface temperature is given by

$$T_S = \frac{p}{2K} \left( \sqrt{(D^2 + (2d)^2) - 2d} \right) \tag{A5}$$

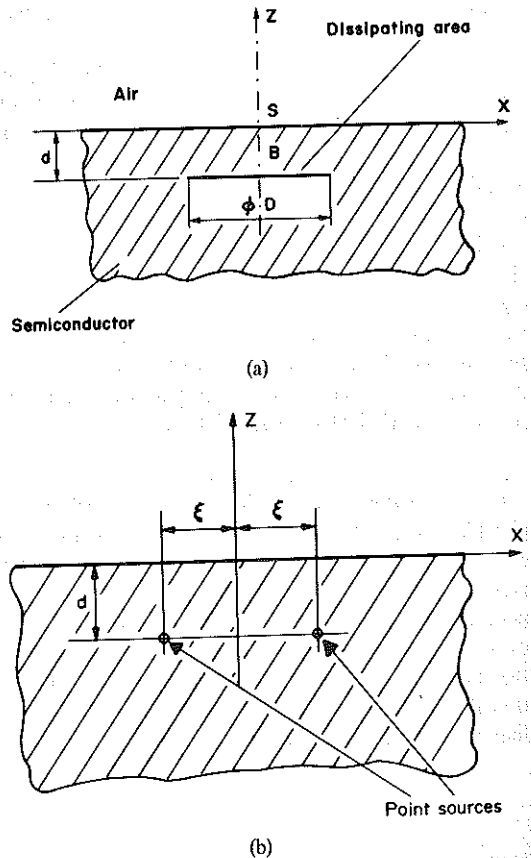


Fig. 7. Explanatory illustrations for calculations of the error and resolution of the liquid crystal thermographical method used for multilayer electronic devices. (a) Semiconductor bulk containing a circular dissipation area with diameter *D* at depth *d* from the surface. The *x*-axis is at the sample surface. Point *B* is at the centre of the circular area, point *S* is above it at the sample surface. (b) Two point-like heat sources in the bulk of the semiconductor at depth *d* from its surface. The points are at a distance  $2\xi$  from each other.

referring to point *S*. Thus, the error in measuring the maximum temperature is

$$\Delta T = \frac{p}{2K} \left( \frac{D}{2} + \sqrt{\left(\left(\frac{D}{2}\right)^2 + (2d)^2\right)} - \sqrt{(D^2 + (2d)^2)} \right) \quad (\text{A6})$$

Let us consider as an example the case in which the dissipation density  $p = 10^7 \text{ W/m}^2$  (this value is about the allowable maximum),  $K = 110 \text{ W/mK}$  (as for GaP) and  $d = 4 \mu\text{m}$ . In this case the error is negligible, when  $D > 20 \mu\text{m}$  and is only  $0.075^\circ\text{C}$  for a dissipation area with  $D = 8 \mu\text{m}$  dia. and  $0.24^\circ\text{C}$  for  $D = 4 \mu\text{m}$ . Thus, the error of the measured maximum temperatures is fairly small (except for very small heat sources).

*Limit of the resolution.* Two equal point sources ("hot spots") are assumed at a depth  $d$ , with a mutual distance  $2\xi$  (Fig. 7b). We

consider the sources theoretically distinguishable from surface measurements when their surface temperature distribution shows two distinct maxima. The surface temperature distribution along the axis  $x$  is given by

$$T(x) = \frac{1}{2\pi K} \left( \frac{1}{\sqrt{(d^2 + (x - \xi)^2)}} + \frac{1}{\sqrt{(d^2 + (x + \xi)^2)}} \right) \quad (\text{A7})$$

Investigation of this expression shows that the two points are distinguishable (in the above-defined sense) if

$$\xi > 0.7071 d. \quad (\text{A8})$$

This is the theoretical limit of the resolution.